

Numerical Analysis of the Transient Thermal Stress Intensity Factors in Cylinders Containing an External Circumferential Semi-Elliptical Crack

Majid Jamal-Omidi¹, Seyed Mehdi Nabavi^{1*}, Mehrdad Aghanavehsi²

1. Faculty of Aerospace Engineering, Malek-Ashtar University of Technology, Tehran, Iran

2. Department of Mechanical Engineering, College of Engineering, Islamic Azad University, Tehran, Iran

Corresponding author: nabavi@mut.ac.ir

ARTICLE INFO

Article history:

Received: 14 September 2021

Revised: 05 January 2022

Accepted: 20 April 2022

Keywords:

External semi-elliptical circumferential crack;
Transient thermal stress;
Three-dimensional finite element method;
Stress intensity factors;
Cylinder.

ABSTRACT

In this paper, the transient thermal stress intensity factors for circumferential semi-elliptical crack located on the external surface of the cylinder are determined numerically. The internal surface of the cylinder is exposed to ultra-cold fluid, and the external wall is kept at a constant temperature. The three-dimensional finite element method in ABAQUS software and singular elements in the crack front has been used. In order to ensure the accuracy of the modelling process, stress intensity factors on the cylinder containing the semi-elliptical crack under mechanical loading for different geometric dimensions of the cylinder are extracted, and the results are evaluated with available data. In the research process, transient thermal stress has been modelled using an uncoupled thermoelasticity model in the quasi-static state. Also, the thermal stress results in steady-state are compared to the existing analytical data and, excellent agreement is achieved. Finally, transient thermal stress intensity factors are presented for different values of cylinder radius ratio and various relative depths and aspect ratios of the crack.

1. Introduction

Thin and thick-walled cylinders are one of the most widely used and common structures in the industry, which are generally subjected to mechanical, thermal and vibration loads. As a result of applying these types of loads and their persistence, the possibility of

defects and cracks increases, so that cracks are nucleated on the plane of maximum normal stress in the internal and external surfaces and with changes in thermal loads, thermo-mechanical stresses around the crack tip increase which may lead to crack growth and eventually structural failure. Accordingly, these types of structures will

How to cite this article:

Jamal-Omidi, M., Nabavi, S., Aghanavehsi, M. (2023). Numerical Analysis of the Transient Thermal Stress Intensity Factors in Cylinders Containing an External Circumferential Semi-Elliptical Crack. *Journal of Rehabilitation in Civil Engineering*, 11(1), 127-140. <https://doi.org/10.22075/JRCE.2022.24540.1553>

have a limited life, and determining their fatigue life is very important because the correct estimation of fatigue life can prevent the occurrence of catastrophes and irreparable financial and human losses. So in the assessment of fatigue life estimation through fracture mechanics, it is necessary to determine the stress intensity factor (SIF) parameter. Among the different types of cracks in cylinders under pressure and heat, two types of cracks, including longitudinal and circumferential surface cracks, which occur mainly in the welding seam, will have the most sensitive and critical condition. This phenomenon mainly occurs in pipes exposed to corrosive environments. Irregular geometric defects become semi-elliptical cracks over time [1], so it is imperative to investigate the SIF to evaluate cracks growth in such cylinders.

Raju and Newman [2] calculated the SIFs for the circumferential semi-elliptical surface cracks in the pipes and rods in both tensile and flexural loading states using the finite element method (FEM). Carpinteri et al. [3-6] employed the same crack and solution method to study crack growth under axial and flexural cyclic loads. Ligoria et al. [7] modelled and analyzed the external circumferential semi-elliptical crack growth in a hollow cylinder under cyclic flexural loading using the FEM. Shahani and Habibi [8] and Shahani et al. [9] also analyzed the problem using the FEM and experimental test by adding torsion to the previous loads. Fillery and Hu [10], Ghajar et al. [11], Abbaspour Niasani et al. [12] and Nabavi et al. [13] used the weight function method to study the external circumferential crack under steady-state thermal loading.

Fakhri et al. [14] extracted the stress intensity factors for the thin-walled cylinder

containing external and internal circumferential semi-elliptical crack under tensile and internal pressure loads using the FEM. Al-Moayed et al. [15,16] presented SIFs for a thick-walled cylinder containing external and internal semi-elliptical crack under both pure mode I and mixed-mode. Qian and Li [17] evaluated the effect of residual stress due to welding on the internal circumferential semi-elliptical crack behavior in the cylinder using ABAQUS software. Miyazaki and Mochizuki [18] investigated the effects of two types of stress distributions due to weld connection on the SIF at the deep point of the semi-elliptical crack located in the cylinder and sheet using the SIF solution in API 579-1 standard. Zareei and Nabavi [19, 20] and Nabavi and Shahmorady [21] used the weight function method to investigate the circumferential semi-elliptical cracks located on the internal surface of the cylinder under different loads, including residual stress due to welding. They also compared the results with the finite element analysis. Paarmann and Sander [22] obtained numerically and analytically the thermal SIFs for a thick-walled sheet and cylinder containing circumferential semi-elliptical cracks under the cyclic thermal load whose temperature decreases during the cooling process from 545 to 50 °C in 180 to 3600 s.

Based on the studies performed, it was observed that most researchers examined the circumferential semi-elliptical cracks under steady-state thermo-mechanical loads. Furthermore, the effect of time is not considered in the residual stress analysis due to welding. The complexity of FE modeling in circumferential semi-elliptical cracking is more significant than its longitudinal type. On the other hand, the time-consuming nature of the transient thermal analysis makes it difficult to find a straightforward

solution to this type of problems. In this paper, the circumferential semi-elliptical crack is considered on the external surface of the cylinder. This type of crack usually occurs in the circumferential welding seams of pipes exposed to corrosion by the surrounding environment. In the research process, the SIFs of mode I for thin and thick wall cylinders at the deepest point of the crack under transient thermal loading have been calculated using the 3D FEM and singular elements in the crack front for different values of cylinder radius ratio, relative depth and crack aspect ratio. In this regard, at first, the variations of SIFs for the mechanical loading state are extracted, and the obtained results are validated with the available data in order to ensure convergence and elemental accuracy. Then transient thermal stress distributions in the cylinder without cracks are verified. Finally, the transient thermal SIFs for different states of cylinder and crack are calculated and assessed.

2. Crack geometry and mechanical and thermal characteristics

In order to study the behavior of a circumferential semi-elliptical crack located on the external surface of an isotropic cylinder carrying ultra-cold fluid, the three-dimensional FEM (ABAQUS software) is used. In order to neglect the effect of edges on SIFs, the plane strain assumption is adopted (Fig. 1). The thermo-mechanical properties of the material are listed in Table 1. Conductive heat transfer, which is applied due to super cool fluid flow into the internal cylinder wall, makes the thermal field. Transient thermal field changes and making tensile and compressive stress around the crack tip reasonably infer increased crack

growth. In order to estimate transient thermal SIFs using FE analysis, first temperature field distribution is obtained using uncoupled thermoelasticity analysis separately. Then quasi-static thermal stress resulting from this field was determined using singular elements in the cracked cylinder. Then the transient thermal SIFs at the deepest point of crack, which is demonstrative of the maximum crack front penetration to the cylinder wall, are extracted for different values of cylindrical radius ratio ($R_o/R_i = 1.1, 1.25$ and 2), various values of relative depth ($0.2 \leq a/B \leq 0.8$), and aspect ratio ($0.2 \leq a/c \leq 1$).

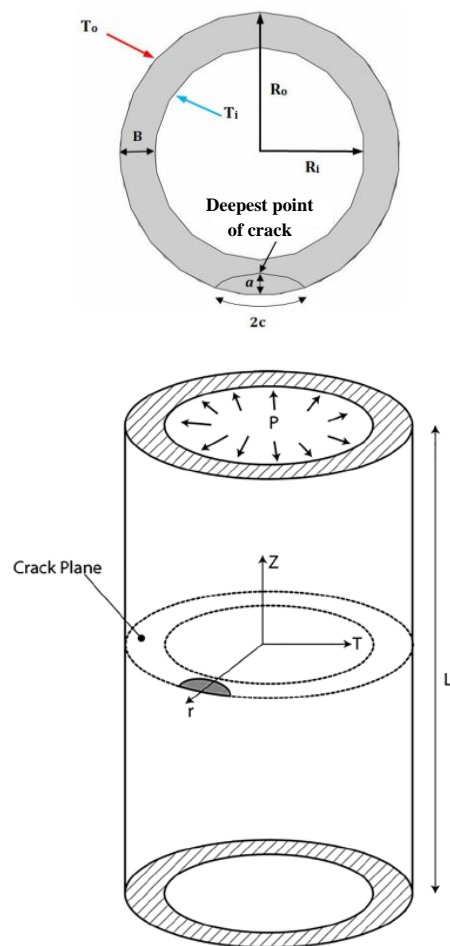


Fig. 1. Geometry and parameters of the external semi-elliptical circumferential crack.

Table 1. The properties of the cylinder's material.

Parameter	Unit	Value
Density	kg/m ³	7600
Young's modulus	GPa	200
Poisson's ratio	-	0.3
Linear thermal expansion coefficient	1/°K	12×10 ⁻⁶
Thermal conductivity	W/m.°K	25

3. Three-dimensional finite element modeling

In the simulation process, the crack and its surroundings in one part and other parts of the cylinder have been separately modeled with radius ratios of 1.10, 1.25 and 2 (see Fig. 2a). This radial ratio covers a wide range of thin and thick-walled industrial cylinders. In order to prevent the edge effects and apply plane strain conditions, the end of the cylinder is fixed in the longitudinal direction, and its length is considered to be 10 times larger than the internal radius.

As shown in Fig. 1, due to two planes of symmetry, crack plane (r-T) and perpendicular to it at the deepest point (r-Z), a quarter of the model can be used in the three-dimensional analysis, which reduces the computational cost and memory usage for the analysis of finite element model. In the meshing process, three-dimensional isoparametric elements and their singular form (C3D15 element and DC3D15 element, respectively) at the crack tip is utilized for mechanical and thermal loads. In other areas, 20-node 3D hexahedral elements C3D20R/DC3D20 and 8-node 3D hexahedral elements C3D8R/DC3D8 are employed for mechanical and thermal loading conditions. Assuming the linear elastic fracture mechanics (LEFM) theory, middle nodes of wedge elements are placed in one fourth distance from the crack tip to make stresses singularity in crack front that Fig. 2b shows the place of these nodes. In each analyzes, the convergence of the results and the

meshing accuracy are examined, ensuring its accuracy. The effect of the number of elements on the value of the SIF for a relative depth and specific aspect ratio is given in Table 2.

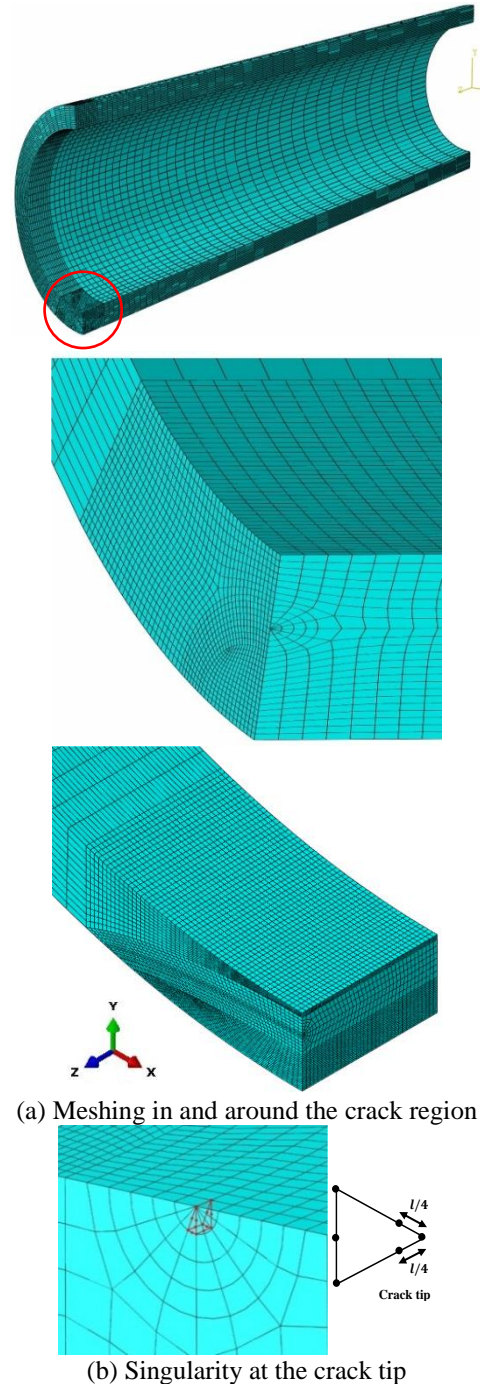


Fig. 2. Three-dimensional finite element modeling for an external circumferential semi-elliptical crack.

Table 2. Mesh convergence for modeling a homogeneous cylinder containing circumferential semi-elliptical crack.

Number of elements	SIF (K_I)
1225	1.1050×10^7
1880	1.1047×10^7
4010	1.1041×10^7
10700	1.1035×10^7
29120	1.1030×10^7
35117	1.1029×10^7
52000	1.1029×10^7

There are three displacement extrapolation, stiffness derivative, and J-integral methods to calculate the values of mode I SIFs, and each of them has its own advantages and disadvantages [23]. The J-integral method is useable in two- and three-dimensional cracks. Considering the nature of the deepest point of the semi-elliptical crack, after calculating the J-integral, mode I SIF (which shows plane strain nature on the crack front) is determined using Equation (1) as follows [24]:

$$K_I = \sqrt{EJ/(1 - \nu^2)} \tag{1}$$

where E and ν are elastic modulus and Poisson's ratio, respectively. J-value is the average contours around the crack's deepest point on the plane perpendicular to the crack front. For analysis, the cylinder containing a circumferential semi-elliptical crack located outside the cylinder is subjected to a uniform tensile load in the longitudinal direction. SIFs are calculated for a wide range of cylinder geometry, with cylinder radius ratios of $R_o/R_i = 1.10, 1.25, \text{ and } 2$, aspect ratio $a/c = 0.6 \text{ to } 1.0$, and crack relative depth ratio $a/B = 0.2 \text{ to } 0.8$ to validate the results of the three-dimensional simulation. The applied

mechanical properties are given in Table 1. The results are dimensionless through Equation (2).

$$K_{NU} = K_I/\sigma_0\sqrt{\pi a/Q} \tag{2}$$

where σ_0 and Q are the uniform tensile stress and the geometrical parameter of the crack, respectively. Parameter Q is calculated through elliptical integral series expansion and using relation 3 [24]:

$$Q = 1 + 1.464(a/c)^{1.65}, a/c \leq 1 \tag{3}$$

The results of dimensionless SIFs compared with available data are given in Tables 3 to 5. The results show that the modeling and simulation of the present work have high accuracy.

Table 3. Comparison of dimensionless SIFs under axial tension for radius ratio 1.10.

a/c	a/B	Present	Raju and Newman [2]	Fakhri et al. [14]	API 579 [25]	Laham [26]	Bergman [27]
0.6	0.2	0.90	1.10	0.85	-	-	-
	0.8	1.24	1.25	1.24	-	-	-
0.8	0.2	1.06	-	1.05	-	-	-
	0.8	1.16	-	1.25	-	-	-
1.0	0.2	1.04	1.02	1.04	1.05	1.04	1.04
	0.4	1.06	-	-	1.08	1.06	1.05
	0.6	1.09	-	-	1.10	1.08	1.08
	0.8	1.11	1.07	1.35	1.11	1.09	1.08

Table 4. Comparison of dimensionless SIFs under axial tension for radius ratio 1.25.

a/c	a/t	Present	Raju and Newman [2]	Al-Moayed et al. [14]
0.6	0.2	1.076	1.101	0.955
	0.8	1.251	1.285	1.055
0.8	0.2	1.057	-	1.050
	0.8	1.174	-	1.350
1.0	0.2	1.040	1.019	1.110
	0.8	1.120	1.072	1.355

Table 5. Comparison of dimensionless SIFs under axial tension for radius ratio 2.0.

a/c	a/t	Present	Raju and Newman [2]	API 579 [25]
0.6	0.2	1.077	1.113	-
	0.8	1.387	1.455	-
1.0	0.2	1.043	1.015	-
	0.4	1.075	-	1.027
	0.6	1.123	-	1.050
	0.8	1.107	1.076	1.051

4. Thermal and stress distribution in cylinder without crack

4.1 Governing equations of thermoelasticity

The governing equations of uncoupled thermoelasticity in the quasi-static state for homogeneous cylinder assuming axisymmetry and regardless of producing internal heat and body forces are defined as follows [28]:

$$\frac{\partial^2 T}{\partial r^2} + \frac{1}{r} \frac{\partial T}{\partial r} = \frac{1}{\alpha^*} \frac{\partial T}{\partial t} \quad (4)$$

$$\frac{\partial^2 u}{\partial r^2} + \frac{1}{r} \frac{\partial u}{\partial r} - \frac{u}{r^2} - \frac{\alpha(3\lambda + 2\mu)}{\mu} \frac{\partial T}{\partial r} = 0 \quad (5)$$

where α and α^* are linear thermal expansion factor and thermal diffusivity coefficients, respectively. Furthermore, λ and μ are Lamé

constants. Determination of thermal distribution and displacement by applying boundary and initial conditions is the primary aim of a thermoelasticity problem. In coupled thermoelasticity, the governing equations are dependent because of the thermal field's effect on the displacement equation and also the mechanical dissipation on the heat equation. If the boundary condition is of thermal shock type, the analyzes should be accomplished based on coupled solution, and the effect of thermoelastic shock wave propagation should be assessed.

On the other hand, the effect of wave propagation is neglected and the inertia term is removed in the quasi-static solution. If the temperature distribution in the body is applied continuously and slowly, in this case, the effect of coupling terms can be ignored and the equations are analyzed in an uncoupled manner (Equations (4) and (5)). Considering that the distribution of longitudinal stress due to internal pressure in the cylinder creates a behavior similar to uniform tension in circumferential cracks, consequently, in this study, the pure thermal stress is determined and evaluated. Apparently, if the cylinder is also under internal pressure in addition to the thermal load, the SIFs can be added together using the superposition principle. Accordingly, in this paper, only constant thermal boundary conditions are considered prescribed on the inner and outer surfaces, and all the steps and conditions mentioned in Equations (4) and (5) are in the form of uncoupled quasi-static thermoelasticity. In this way, at first, the transient thermal distribution in the cylinder is calculated separately (Equation (4)) and then the results of thermal stress due to the thermal field are determined. Following, the transient thermal SIFs for cylinder containing circumferential semi-elliptical crack are

obtained using the J-integral method. It should be noted that the thermo-mechanical properties of the material are assumed to be constant and independent of temperature in all analyses.

4.2 Thermo-mechanical response in homogeneous cylinder

As mentioned, in order to determine the transient thermal SIFs, the transient thermal distribution due to uncoupled loading should be first determined and considered an input in thermal stress analysis. For this purpose, the transient thermal distribution in the internal and external walls of the cylinder for radius ratios (R_o/R_i) 1.1, 1.25, and 2.0 are numerically extracted. The transient temperature and stress distributions are dimensionless using Equations (6) and (7).

$$T_n = (T(r, t) - T_i)/(T_o - T_i) \tag{6}$$

$$\sigma_n = \frac{\sigma_z(r, t) (1 - \nu)}{E\alpha(T_o - T_i)} \tag{7}$$

where $T(r, t)$ and $\sigma_z(r, t)$ are temperature and longitudinal stress fields in the cylinder without cracks, respectively. The time effect is also determined in the form of the Fourier number (Fo).

$$Fo = \alpha t/R_o^2 \tag{8}$$

where t , α and R_o are time, linear thermal expansion coefficient, and cylinder external radius, respectively.

The transient temperature and stress distributions in the cylinder without crack for a radius ratio of 1.10 compared to the available analytical solution in the steady-state [29] are shown in Figs. 3 and 4. As can be seen, with increasing the Fourier number

and time passes make the gradient of changes in diagrams decreases, and the solution tends to the steady-state.

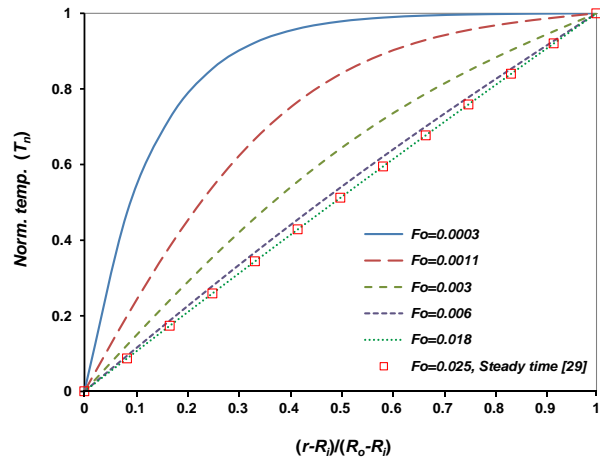


Fig. 3. Transient temperature distribution along the thickness of the cylinder for a radius ratio of 1.1 at specified times.

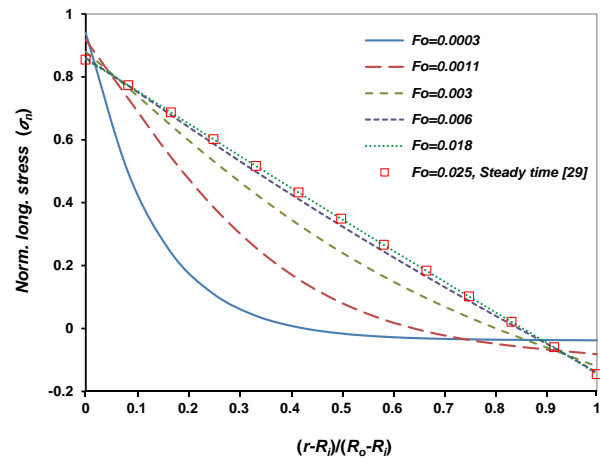


Fig. 4. Longitudinal transient thermal stress distribution along the thickness of the cylinder for a radius ratio of 1.1 at specified times.

5. Results and discussion

The steady thermal SIFs for the homogeneous cylinder containing an external circumferential semi-elliptical crack are extracted for radius ratio of 1.10, the aspect ratio of $0.2 \leq a/c \leq 1.0$, and the relative crack

depth of $0.2 \leq a/B \leq 0.8$. The thermal and mechanical properties of Table 1 are exploited. The problem is analyzed by the uncoupled quasi-static solution method, and the boundary conditions of the type of conductive heat transfer and super cool fluid flow with temperatures of -100 and 0 °C in the internal and external cylinder surfaces are considered. In the following, longitudinal stress due to thermal boundary conditions causes the opening of the external circumferential crack in the opening mode. Furthermore, the thermal SIFs obtained from the FE solution become dimensionless as follows

$$K_{NT} = \frac{K_I}{E\alpha\Delta T\sqrt{\pi a}} \quad (9)$$

In the internal surface of the cylinder, with increasing ultra-cold flow, Temperature reduction is transferred from the internal wall to the outer one (according to Fig. 4) and causes compressive stress across the external part of the cylinder. This phenomenon leads to the closing of the crack mouth. Considering that it is possible to employ the superposition principle in combining loadings in cracked problems, so according to Fig. 5, the negative values of SIFs are also represented in low relative depth. According to the diagram, with increasing relative depth and changing the nature of stress behaviour in the cylinder, the crack changes to the opening mode. So that with increasing the relative crack depth the values of the SIFs increase, while with increasing the aspect ratio, the rate of decrease of the values is observed.

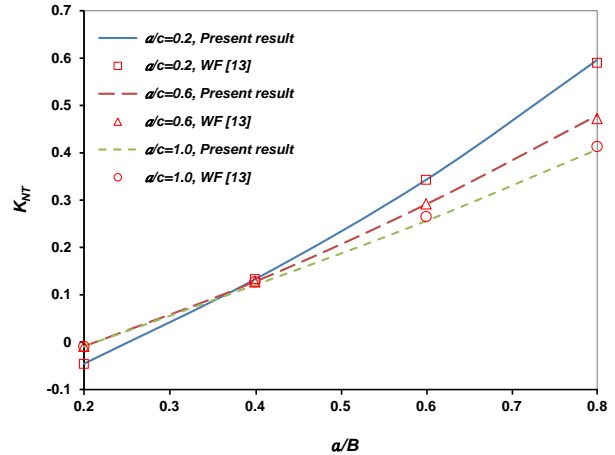


Fig. 5. Steady normalized thermal SIFs for radius ratio of 1.1.

In general, more circular cracks at lower relative depths are more critical, and semi-elliptical cracks are more critical at higher relative depths. Furthermore, to ensure the accuracy of the present analysis, the thermal SIFs resulting from the ratio of radius to thickness 10 are compared with the available data obtained from the weight function method [13], and a good agreement is achieved.

In the following, the results of transient thermal SIFs for cylinder containing an external circumferential semi-elliptical crack at the deepest point up to steady time for different radius ratios (1.1, 1.25, and 2.0) and based on relative depth for each aspect ratio are indicated in Figs. 6 to 14.

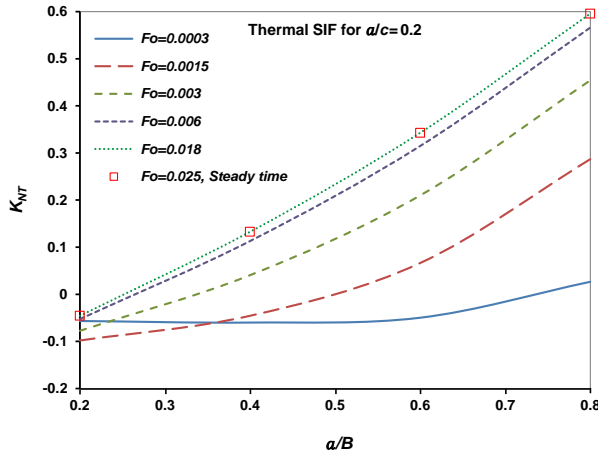


Fig. 6. Variation of dimensionless transient thermal SIFs for radius ratio of 1.1 and aspect ratio of 0.2.

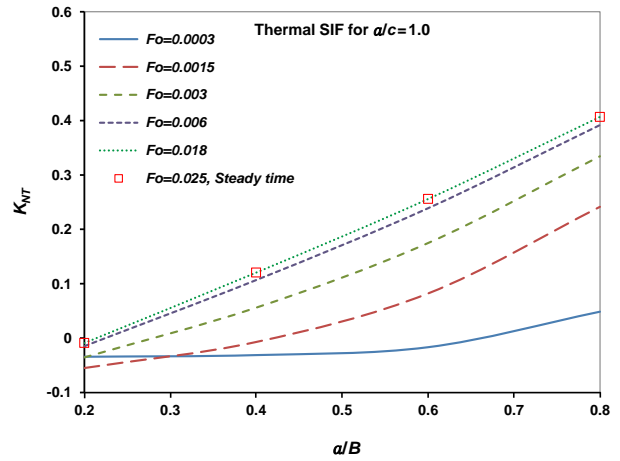


Fig. 8. Variation of dimensionless transient thermal SIFs for radius ratio of 1.1 and aspect ratio of 1.0.

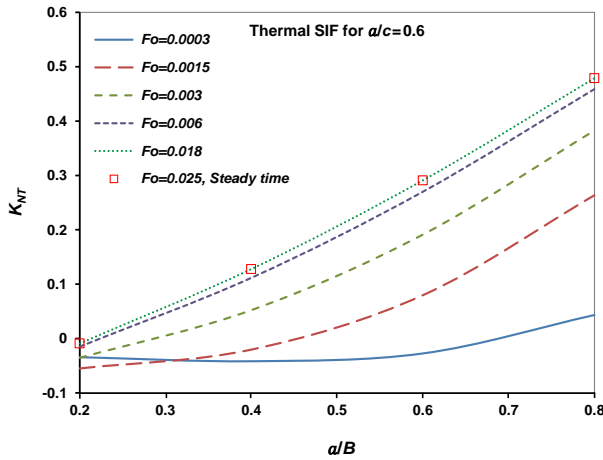


Fig. 7. Variation of dimensionless transient thermal SIFs for radius ratio of 1.1 and aspect ratio of 0.6.

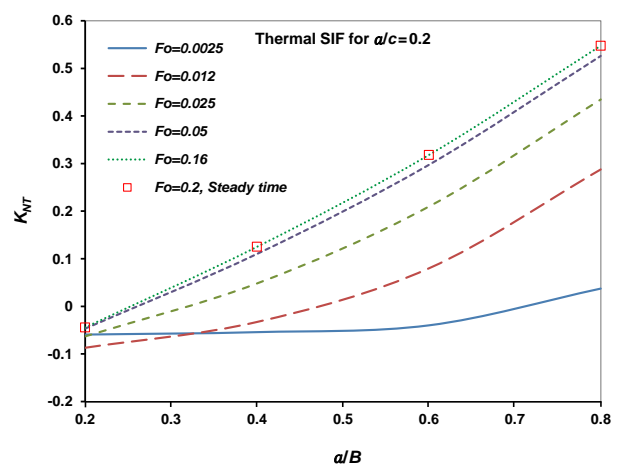


Fig. 9. Variation of dimensionless transient thermal SIFs for radius ratio of 1.25 and aspect ratio of 0.2.

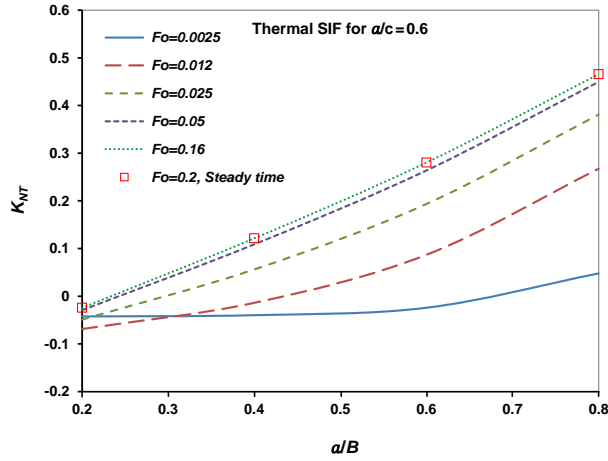


Fig. 10. Variation of dimensionless transient thermal SIFs for radius ratio of 1.25 and aspect ratio of 0.6.

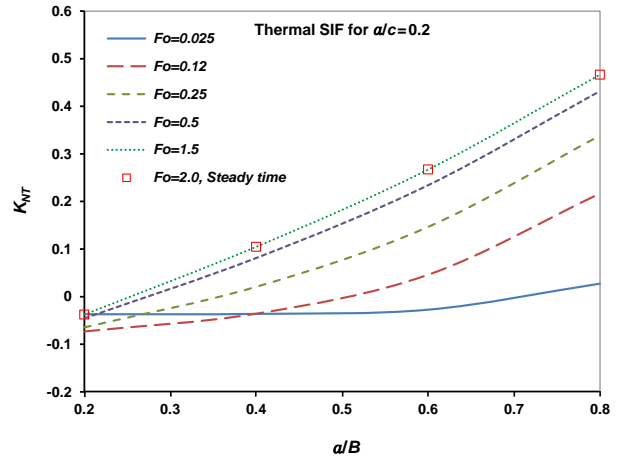


Fig. 12. Variation of dimensionless transient thermal SIFs for radius ratio of 2.0 and aspect ratio of 0.2.

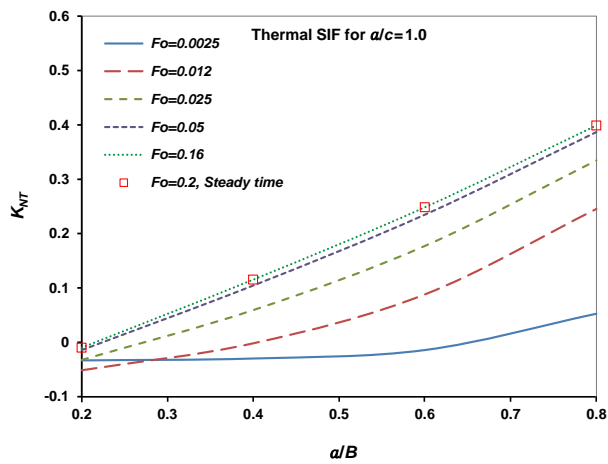


Fig. 11. Variation of dimensionless transient thermal SIFs for radius ratio of 1.25 and aspect ratio of 1.0.

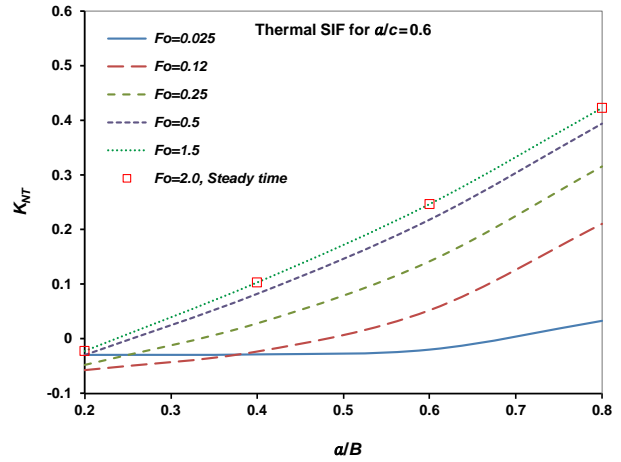


Fig. 13. Variation of dimensionless transient thermal SIFs for radius ratio of 2.0 and aspect ratio of 0.6.

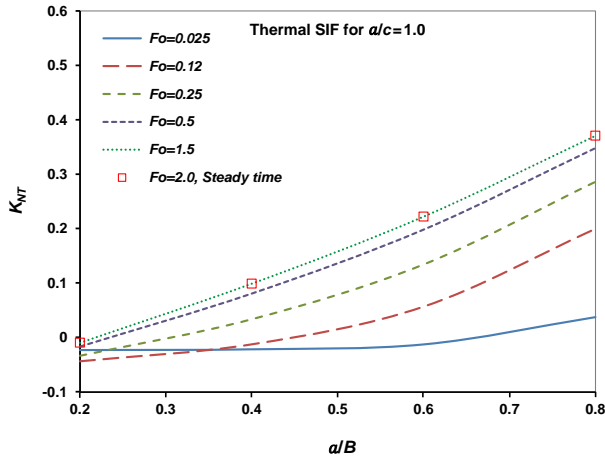


Fig. 14. Variation of dimensionless transient thermal SIFs for radius ratio of 2.0 and aspect ratio of 1.0.

According to the obtained results, the thermal SIFs in the cylinder with a radius ratio of 1.1 in $Fo = 0.025$ and other radius ratios in $Fo = 0.25$ and $Fo = 2$, respectively, have reached steady values. Also, with increasing Fourier number (Fo) and the passage of time, thermal SIFs demonstrate an increasing trend so that the maximum value of SIFs occur for all three radius ratios in all aspect ratios and relative depths at the steady time. SIFs do not change from the negative state almost for all three radius ratios and different aspect ratios at a relative depth of 0.2 and over time, the crack opening displacement will permanently be closed due to the compressive stress distribution in the cylinder external wall. In other words, growth for this type of crack is not critical up to 20% thickness. Also, the increase in the SIFs at higher relative depths over time is observed in different aspect ratios. Moreover, for all cylinders at a relative depth of 0.8 and aspect ratio of 0.2 where the crack is semi-elliptical and elongated, the SIF reaches the highest and most critical value possible after stabilizing both thermal and stress distribution. Therefore, when the crack penetration

reaches more than 20% of the critical thickness, the SIFs increase and the crack expands with increasing relative depth.

The SIFs versus the Fourier number (Fo) for all three radius ratios are shown in Figs. 15 to 17. In all three cases in the relative depth range of 0.4, sudden variations and increase in SIFs are observed due to the onset of heat diffusion in the cylindrical wall and the creation of tensile and compressive stress regions. Also, as the thickness of the cylinder increases, the SIF decreases for all aspect ratios and relative depths, and the time to achieve steady state increases. In general, during thermal stress distribution time, more circular cracks with less relative depth are critical, and semi-elliptical cracks with more relative depth are critical. In conclusion, it is necessary to mention that with a 10 times increase in the cylinder wall thickness, a slight percentage decrease in the values of the SIFs occurs, which indicates that increasing the thickness is not cost-effective to prevent the growth of this type of crack in cylinders under pressure and temperature conditions.

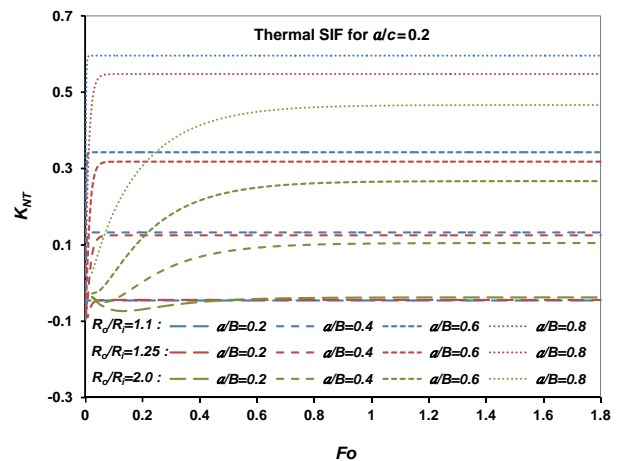


Fig. 15. Variation of transient thermal SIFs versus Fourier number (Fo) for different radial ratios and aspect ratio of 0.2.

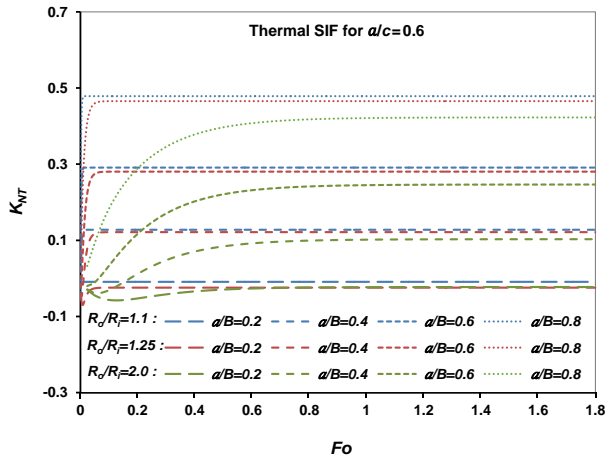


Fig. 16. Variation of transient thermal SIFs versus Fourier number (Fo) for different radial ratios and aspect ratio of 0.6.

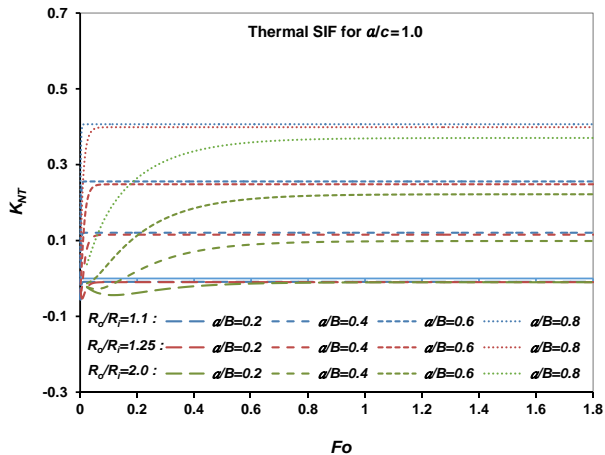


Fig. 17. Variation of transient thermal SIFs versus Fourier number (Fo) for different radial ratios and aspect ratio of 1.0.

6. Conclusions

The paper aims to determine the mode I SIFs for an external circumferential semi-elliptical crack in the cylinder with radius ratios of $R_o/R_i=1.10$, 1.25, and 2.0, aspect ratio $a/c=0.2$ to 1.0, and relative crack depth ratio $a/B=0.2$ to 0.8 under mechanical and transient thermal loading conditions using FEM. In order to ensure the simulation process, first, the results of SIFs in a cracked

cylinder under uniform mechanical loading are evaluated with the current results, and appropriate adaptation is obtained. The following analysis of pure temperature distribution and thermal stress is performed uncoupled for the steady-state and transient state in the cylinder without cracks. Finally, transient thermal SIFs are extracted for a homogeneous cylinder containing an external circumferential semi-elliptical crack. The most important results of the present study are:

- In a homogeneous cylinder containing an external circumferential semi-elliptical crack, the crack tends to grow when the inner surface of the cylinder is colder than its outer one. This phenomenon is due to the nature of the transient tensile thermal stress.
- Thermal SIFs achieve their steady-state values over time, while the maximum thermal SIFs occur. In other words, evaluation based on steady-state values supplies conservative results.
- Thermal SIFs in thin-walled cylinders reach their steady-state faster than thick-walled cylinders. Furthermore, the gradient of transient thermal SIFs in thick-walled cylinders is less than that of thin-walled cylinders.
- Transient thermal SIFs increase with increasing relative crack depth over specified periods of time. In deep cracks, elliptical cracks (with a low aspect ratio) are more critical than circular ones. Circular cracks (with a high aspect ratio) are more critical in shallow cracks.
- As the radius ratio of the cylinder increases, the values of the transient thermal SIFs decrease. Therefore, crack growth occurs quickly in thin-walled cylinders.

- The shallow cracks start closing during the time. In other words, growth for this type of crack up to 20% thickness is not critical. However, when the crack penetration reaches more than 20% of the critical thickness, with increasing relative depth and decreasing aspect ratio, the SIFs increase and the crack expands.
- Increasing the thickness of the cylinder decreases the SIFs over time but merely delays the crack growth rate. Therefore, in this type of cylinders that are prone to such cracks and damages, strengthening and amplification properties should be done using methods such as thermal operations, hardening, reinforcement using composite patches, and other reinforcement procedures in advance.

REFERENCES

- [1] X. B. Lin, R. A. Smith, (1998). Fatigue growth prediction of internal surface cracks in pressure vessels. *Journal Pressure Vessel Technology*, ASME, 120:17–23. doi: 10.1115/1.2841878
- [2] Raju, I.S., Newman, J.C. (1986). Stress intensity factors for circumferential surface cracks in pipes and rods. In *Fracture Mechanics: Seventeenth Volume*, ed. J. Underwood, R. Chait, C. Smith, D. Wilhem, W. Andrews, and J. Newman (West Conshohocken, PA: ASTM International), 789–805. Doi:10.1520/STP17428S
- [3] Carpinteri, A., Brighenti R., Spagnoli, A. (1998). Part-through cracks in pipes under cyclic bending. *Nuclear Engineering and Design*. 185:1–10. doi:10.1016/S0029-5493(98)00189-7
- [4] Carpinteri, A., Brighenti R., (1998). Circumferential surface flaws in pipes under cyclic axial loading. *Engineering Fracture Mechanics*. 60:383–396. Doi:10.1016/S0013-7944(98)00036-8
- [5] Carpinteri, A., Brighenti R., Spagnoli, A. (2000). External surface cracks in shells under cyclic internal pressure. *Fatigue Fracture Engineering Materials and Structures*. 23:467–476. Doi:10.1046/j.1460-2695.2000.00320.x
- [6] A. Carpinteri, R. Brighenti and S. Vantadori, (2003). Circumferentially notched pipe with an external surface crack under complex loading. *International Journal of Mechanical Sciences*. 45:1929–1947. Doi:10.1016/j.ijmecsci.2004.02.007
- [7] Ligorja, S.A., Knight G.S., Ramachandra Murthy, D.S., (2005). Three-dimensional finite element analysis of a semi-elliptical circumferential surface crack in a carbon steel pipe subjected to a bending moment. *Journal of Strain Analysis*. 40:525–533. Doi:10.1243/030932405X16052
- [8] Shahani, A.R., Habibi, S.E. (2007). Stress intensity factors in hollow cylinder containing a circumferential semi-elliptical crack subjected to combined loading. *International Journal of Fatigue*. 29:128–140. Doi:10.1016/j.ijfatigue.2006.01.017
- [9] Shahani, A.R., Mohammadi Shodja M., Shahhosseini, A. (2010). Experimental investigation and finite element analysis of fatigue crack growth in pipes containing a circumferential semi-elliptical crack subjected to bending. *Experimental Mechanics*. 50:563–573. Doi:10.1007/s11340-009-9229-6
- [10] Fillery, B.P. Hu, X.Z. (2012). Compliance based assessment of stress intensity factor in cracked hollow cylinders with finite boundary restraint: Application to thermal shock part II. *Engineering Fracture Mechanics*. 79:18–35. Doi:10.1016/j.engfracmech.2011.09.011
- [11] Ghajar, R., Abbaspour Niasani M., Saeidi Googarchin, H., (2014). Explicit expressions of stress intensity factor for external semi-elliptical circumferential cracks in a cylinder under mechanical and thermal loads. *Modares Mechanical Engineering*. 14:90-98. (In Persian)
- [12] Abbaspour Niasani M., Ghajar, R., Saeidi Googarchin, H., Sharifi, S.M.H., (2017).

- Crack growth pattern prediction in a thin walled cylinder based on closed form thermo-elastic stress intensity factors. *Journal of Mechanical Science and Technology*. 31:1603–1610.
Doi:10.1007/s12206-017-0307-x
- [13] Nabavi, S.M., Montazer Torbati, E., Jamal-Omidi, M. (2020). Weight function for an external circumferential semielliptical crack in a cylinder. *Fatigue Fracture Engineering Materials and Structures*. 43:1487–1499. doi:10.1111/ffe.13224
- [14] Fakhri, O.M., Kareem, A.K., Ismail, A.E., Jamian, S., Nemah, M.N., (2019). Mode I SIFs for internal and external surface semi-elliptical crack located on a thin cylinder. *Test Engineering and Management*. 81:586–596.
- [15] Al-Moayed, O.M., Kareem, A.K., Ismail, A.E., Jamian, S., Nemah, M.N., (2019). Distribution of Mode I stress intensity factors for single circumferential semi-elliptical crack in thick cylinder. *International Journal of Integrated Engineering*. 11:102–111.
- [16] Al-Moayed, O.M., Kareem, A.K., Ismail, A.E., Jamian, S., Nemah, M.N., (2020). Influence coefficients for a single superficial cracked thick cylinder under torsion and bending moments. *International Journal of Integrated Engineering*. 12:132–144.
- [17] Qian, X., Li, T., (2010). Effect of residual stresses on the linear-elastic KI-T field for circumferential surface flaws in pipes. *Engineering Fracture Mechanics*. 77:2682–2697.
Doi:10.1016/j.engfracmech.2010.06.014
- [18] Miyazaki, K., Mochizuki, M., (2011). The effects of residual stress distribution and component geometry on the stress intensity factor of surface crack. *Journal of Pressure Vessel Technology*. 133:1–7.
Doi:10.1115/1.4002671
- [19] Zareei, A., Nabavi, S.M., (2016). Weight function for circumferential semi-elliptical cracks in cylinders due to residual stress fields induced by welding. *Archive of Applied Mechanics*. 86:1219–1230.
Doi:10.1007/s00419-015-1087-3
- [20] Zareei, A., Nabavi, S.M., (2016). Calculation of stress intensity factors for circumferential semi-elliptical cracks with high aspect ratio in pipes. *International Journal of Pressure Vessels and Piping*. 146:32–38.
Doi: 10.1016/j.ijpvp.2016.05.008
- [21] Nabavi, S.M., Shahmorady, M.B. (2020). Stress intensity factors for circumferential semi-elliptical cracks in cylinders subjected to forced convection heat transfer. *International Journal of Integrated Engineering*. 12:232–239.
- [22] Paarmann, M., Sander, M., (2020). Analytical determination of stress intensity factors in thick walled thermally loaded components. *Engineering Fracture Mechanics*. 235, e107125.
Doi:10.1016/j.engfracmech.2020.107125
- [23] Banks-Sills, L., (1991). Application of the finite element to linear elastic fracture mechanic. *Applied Mechanics Review*. 44:447–461. Doi: 10.1115/1.3119488
- [24] Anderson, T.L., (2017). *Fracture Mechanics-Fundamentals and Applications*, 4th Edition, Boca Raton, CRC Press.
- [25] Institute AP. *API 579-1/ASME FFS-1. Fitness-for-service*. 2nd Edition, 2007.
- [26] Laham S. *Stress intensity factor and limit load*. Handbook, British Energy Generation Limited, 1998.
- [27] Bergman, M. (1995). Stress intensity factors for circumferential surface cracks in pipes. *Fatigue Fracture Engineering Materials and Structures*. 18:1155–1172.
Doi:10.1111/j.1460-2695.1995.tb00845.x
- [28] Hetnarski R.B., Eslami M.R. (2019). *Thermal stresses: advanced theory and applications*. 2nd Edition, Springer.
- [29] Alipour, K., Nabavi, S.M., Bakhshan, M., Rahimi, F., Zareei, H., (2013) Thermal stresses solutions in cylinders due to steady state forced convection heat transfer. 13th Conference of Iranian Aerospace Society, Tehran, University of Tehran, Faculty of New Science and Technology.